TU Delft

Delft University of Technology

Modification-free boron-doped diamond as a sensing material for direct and reliable detection of the antiretroviral drug nevirapine

Baluchová, Simona; Mamaloukou, Antigoni; Koldenhof, Rombert H.J.M.; Buijnsters, Josephus G.

DOI
10.1016/j.electacta.2023.142238

Publication date
2023

Document Version
Final published version

Published in
Electrochimica Acta

Citation (APA)
Baluchová, S., Mamaloukou, A., Koldenhof, R. H. J. M., & Buijnsters, J. G. (2023). Modification-free boron-doped diamond as a sensing material for direct and reliable detection of the antiretroviral drug nevirapine. *Electrochimica Acta*, *450*, Article 142238. https://doi.org/10.1016/j.electacta.2023.142238

Important note
To cite this publication, please use the final published version (if applicable).
Please check the document version above.

Copyright
Other than for strictly personal use, it is not permitted to download, forward or distribute the text or part of it, without the consent of the author(s) and/or copyright holder(s), unless the work is under an open content license such as Creative Commons.

Takedown policy
Please contact us and provide details if you believe this document breaches copyrights.
We will remove access to the work immediately and investigate your claim.

This work is downloaded from Delft University of Technology.
For technical reasons the number of authors shown on this cover page is limited to a maximum of 10.

Electrochimica Acta 450 (2023) 142238

Contents lists available at ScienceDirect

Electrochimica Acta

journal homepage: www.journals.elsevier.com/electrochimica-acta

Modification-free boron-doped diamond as a sensing material for direct and reliable detection of the antiretroviral drug nevirapine

Simona Baluchová [a,*], Antigoni Mamaloukou [a,b], Rombert H.J.M. Koldenhof [a], Josephus G. Buijnsters [a,*]

[a] Department of Precision and Microsystems Engineering, Delft University of Technology, Mekelweg 2, 2628 CD Delft, the Netherlands
[b] Department of Chemical Engineering, University of Patras, Caratheodory 1, GR 265 04 Patras, Greece

ARTICLE INFO

Keywords:
Boron-doped diamond
Electrochemical sensor
Nevirapine
Surface pre-treatment
Voltammetry

ABSTRACT

In this work, non-modified boron-doped diamond (BDD) was employed first time ever as the sensing material for the in-depth voltammetric study of the antiretroviral drug nevirapine (NVP) used to treat HIV infections. Two types of electrode surface pre-treatments, anodic oxidation and alumina-polishing, yielded BDD of different surface chemistry, denoted as O-BDD and p-BDD, respectively. Induced alterations in BDD surface composition reflected in distinct voltammetric responses of NVP, also dependant on the pH of the medium. The electrochemical oxidation of NVP on both electrodes, whose mechanism is proposed herein, has an irreversible character and is controlled by diffusion. The analytical figures of merit were assessed in a pH 2.0 buffer on O-BDD, and in supporting electrolytes of pH 5.0 and 13.0 on p-BDD using differential pulse voltammetry. Overall, NVP provided signals of excellent intra- and inter-day repeatability (RSD $\leq$ 5.0%) which remained unaffected even in the presence of common interfering compounds (e.g., glucose, ascorbic acid, uric acid, and dopamine). Even though the O-BDD electrode outperformed the p-BDD electrode in terms of sensitivity and the lowest detection limit achieved (0.04 μM), both O-BDD and p-BDD provided highly favourable analytical parameters fulfilling the requirements for clinical application for NVP sensing and monitoring in biofluids. This was also proved by electroanalysis of NVP in synthetic serum samples where recovery values between 96.3 and 103.0% were successfully achieved. Finally, unique properties of BDD allowed to develop a direct, modification-free, and reliable protocol for NVP detection, which paves the way for the full sensor development.

1. Introduction

Human immunodeficiency virus (HIV) is an enveloped RNA retrovirus harming the cells of the immune system and weakening the body's ability to fight regular infections and diseases. If HIV infection remains untreated, it may progress to acquired immunodeficiency syndrome (AIDS). The antiretroviral therapy employs licensed anti-HIV compounds and one of the most extensively prescribed antiretroviral drugs worldwide is a dipyridodiazepinone inhibitor [1], nevirapine (NVP). NVP readily absorbs (> 90%) after oral intake and is active in the form administrated [2]. NVP undergoes biotransformation via cytochrome P-450 (oxidative) metabolism and only a negligible amount (< 3%) of the total NVP dose is excreted unchanged in urine [2,3]. Consequently, it is of a high importance to monitor the NVP concentration levels in the patient's blood plasma and/or serum to establish the optimum therapeutic dosage to avoid negative effects. Increased levels of NVP and its accumulation can be detected in patients suffering from liver diseases and may manifest via a range of serious side effects, while low plasma concentrations can trigger the development of virus resistance [2]. Besides, anti-HIV agents are used for a life-time and their monitoring is essential to reduce the risk of toxicity [4] and maintain the suitable management of HIV/AIDS infection treatment.

In addition, anti(retro)viral drugs have been recently identified as emerging environmental pollutants in wastewater and more importantly in surface waters [5–7]; in the global study which monitored over 1000 sampling sites in 104 countries of all continents, NVP fell into the group of the 53 most frequently detected pharmaceuticals in world's rivers (33rd place) [8]. This may be related to the fact that NVP is highly resistant against conventional wastewater treatment procedures (e.g., chlorination), and thus persists in effluents and environment [5,6,9].

Evidently, it is crucial to establish suitable procedures for monitoring and detection of NVP in pharmaceutical, clinical (blood serum) and

* Corresponding authors.
E-mail addresses: S.Baluchova@tudelft.nl (S. Baluchová), J.G.Buijnsters@tudelft.nl (J.G. Buijnsters).

https://doi.org/10.1016/j.electacta.2023.142238
Received 10 January 2023; Received in revised form 27 February 2023; Accepted 13 March 2023
Available online 14 March 2023
0013-4686/© 2023 The Author(s). Published by Elsevier Ltd. This is an open access article under the CC BY license (http://creativecommons.org/licenses/by/4.0/).

environmental (surface and waste water) samples. A range of analytical methods has been developed for the NVP determination, including gas chromatography [10], flow injection analysis [11,12], capillary zone electrophoresis [13], high-performance liquid chromatography coupled with UV detection [10,14,15] and (tandem) mass spectrometry [5,7,16,17], matrix-assisted laser desorption/ionized with tandem time-of-flight detector [18], and a fluorescence-based method [19].

Notwithstanding, NVP can undergo electrochemical oxidation [20], thus electroanalytical methods can be favourably used for the monitoring and detection of NVP due to their simplicity, reliability, accuracy, short analysis time, and low-cost, while they still satisfy high requirements on sensitivity and selectivity [21]. Up to date, several electrochemical approaches have been proposed for NVP determination with one common feature: all required electrode surface modification as either none [22,23] or broad, ill-defined and weak NVP peaks were obtained [24–26] on previously employed bare metal and sp^2 carbon-based electrodes. Typically, modifiers such as metallic nanoparticles [27,28], carbon-based nano-sized materials, or their combinations [22,23,25,26,29–31], in some cases synthesized in-house, were employed which make reported modification procedures often multi-step, complex and tedious. Besides, electrografting of an organic molecule [24] on an electrode surface and integration of molecularly imprinted polymers [32,33] has been utilised. Predominantly, common sp^2-carbon-based electrode materials such as glassy carbon [22,26,29–31,33], carbon paste [24,27,32] and graphite [25] served as a support, while a platinum electrode was selected as a transducer in [23].

So far, none of the sensing approaches targeting NVP has utilized sp^3-carbon electrode material, i.e., conductive boron-doped diamond (BDD), despite the fact that BDD has been commonly employed in electroanalysis of pharmaceuticals [34,35] as summarized in recent reviews [36,37], but also in analysis of clinical markers and bio-related compounds [38–41], food products [42,43], pesticides and environmental pollutants [44,45]. BDD-based electrode material possesses a range of unique properties such as (i) exceptionally broad potential window allowing detection of a wide range of analytes, (ii) low and stable background currents, which lead to a higher signal-to-background ratio and thus more sensitive detection ability, (iii) weak molecular adsorption making BDD surface resistant to (bio)fouling and deactivation, which in consequence enables long-term reliability and stability of sensors, and (iv) biocompatibility granting a great potential for biomedical and implantable devices [46,47]. However, these properties and final characteristics of the BDD electrodes are influenced by several factors [46,48], the most significant being boron doping level [49,50], surface termination [51], sp^2-carbon content [40], and crystallographic orientation [51–53].

Alterations in the surface termination along with the type and amount of various surface functional groups affect the electrochemical performance of BDD electrodes towards redox-active analytes, which is then manifested in the changes in the heterogeneous electron transfer (HET) kinetics [54,55] and proclivity to electrode surface (bio)fouling [56,57]. Freshly deposited BDD electrodes are hydrogen (H)-terminated which is associated with the hydrogen-rich atmosphere in the chemical vapour deposition chamber [47,48]. H-termination ($-C^{\delta-}-H^{\delta+}$) makes the BDD surface more conductive, non-polar and hydrophobic, and induces negative electron affinity [58,59]. Several approaches exist with ability to convert H-terminated surface to the oxygen (O)-terminated one, e.g., boiling the BDD electrode in a mixture of concentrated acids, oxygen plasma treatment, and *in-situ* electrochemical anodic oxidation [47,48]. These procedures result in less conductive, polar, hydrophilic O-terminated BDD surfaces ($-C^{\delta+}-O^{\delta-}$) possessing positive electron affinity [58,59]. Electrochemical activation in an anodic regime generates, due to the water oxidation, quasi-free hydroxyl radicals ($^{\bullet}OH$) [46,60] which react with the BDD surface and incorporates oxygen atoms in the form of various functionalities (typically –C–O–C, -C-OH, -C=O, and -COOH) [61,62]. On the other hand, re-hydrogenation of the oxidized surface can be achieved by a reverse process, i.e., electrochemical cathodic reduction leading to the formation of atomic hydrogen, which is able to eliminate oxygen groups from the BDD surface [61,63]. Interestingly, mechanical polishing of the anodically oxidized BDD electrode on alumina slurry results in a complete removal of -COOH groups and a significant decrease in the concentration of other oxygen functionalities (–C-O-C, -C-OH, -C = O) at the diamond surface [62].

In the present study, non-modified BDD electrode was applied for the first time to the voltammetric study of the anti-HIV drug NVP. As illustrated in Scheme 1, the effect of different surface composition of the BDD electrode, induced by selected simple one-step pre-treatment (anodic oxidation vs. alumina-polishing), as well as pH of the analysed solution on the NVP signals was thoroughly examined and elucidated. The nature of NVP electrochemical oxidation on the different BDD surfaces was clarified using cyclic (CV) and linear sweep voltammetry (LSV), while differential pulse voltammetry (DPV) was employed to develop sensitive and reliable methods for NVP detection on both oxidized (O-BDD) and polished (p-BDD) electrodes. The selectivity and applicability of the proposed DPV methods was verified by performing interference study and electroanalysis in synthetic serum samples, respectively.

2. Experimental

2.1. Reagents and solutions

All chemicals, acquired from Sigma-Aldrich and used as-received, were of analytical reagent grade: nevirapine, hexaammineruthenium (III) chloride, potassium hexacyanoferrate(II) trihydrate, glucose, sucrose, ascorbic acid, uric acid, dopamine hydrochloride, alanine, serine, lysine, histidine, phenylalanine, tryptophan, arginine, glycine, tyrosine, aspartic acid, calcium chloride dihydrate, magnesium chloride hexahydrate, sodium phosphate dibasic, phosphate buffered saline (tablets, pH 7.4), sodium chloride, potassium chloride, sodium hydroxide, sulphuric acid (97%), acetic acid, *ortho*-phosphoric acid (85%), boric acid, and ethanol.

The 1 mM stock solution of NVP was prepared in a deionized water-ethanol (1:1) solution and stored in the dark at 4 ± 1 °C. Universal Britton – Robinson (BR) buffers (0.04 M) with pH ranging from 2.0 to 12.0 were prepared by mixing the acidic component (containing *ortho*-phosphoric acid, acetic acid, and boric acid) with 0.2 M sodium hydroxide to achieve required pH value. Acetic buffer of pH 5.0 (0.1 M) and phosphate buffer of pH 2.0 (0.1 M) were prepared by diluting acetic acid and *ortho*-phosphoric acid in deionized water, respectively, and adjusting to the desired pH with the concentrated sodium hydroxide solution.

All aqueous solutions were prepared using ultra-pure water (resistivity of >18.0 MΩ cm), purified with a LWTN Genie A system (Laboratorium Water Technologie Nederland).

2.2. Instrumentation and procedures

All electrochemical measurements were performed in a commercial 20 mL glass electrochemical cell (Bio-Logic, France) at laboratory temperature (23 ± 1 °C) using an Autolab PGSTAT128N controlled by Nova 2.1 software (Metrohm, The Netherlands). A conventional three-electrode set-up was utilised in which a BDD electrode (3 mm diameter, geometrical area, A_{geom}, of 7.1 mm^2, average roughness <10 nm, doping level between 500 and 1000 ppm), silver-silver chloride electrode (Ag|AgCl|3 M NaCl) and a 5.7 cm platinum wire (all provided by Bio-Logic, France) were employed as the working, reference, and counter electrodes, respectively.

The BDD electrode was pre-treated using two procedures, anodic oxidation and mechanical polishing, resulting in different surface termination. To confirm the efficacy of the performed procedures, CVs were recorded in a solution of $[Fe(CN)_6]^{3-/4-}$, a surface sensitive redox marker [54,62]. In general, the electron transfer kinetics of this redox

couple, reflected in peak-to-peak separation (ΔE_p) values, is hindered on the oxidized (O-terminated) surfaces, but facilitated on the polished ones (due to the decrease in the amount of oxygen groups as reported in [62]). The two pre-treatments were executed as follows:

(i) Anodic oxidation was carried out by applying a high positive potential of +2.4 V for 20 min in 0.5 M H_2SO_4 at the beginning of the working day [38,49], which resulted in electrode with oxidized surface, further denoted as O-BDD. Application of high positive potentials initiates water decomposition reaction generating hydroxyl radicals, which react with the BDD surface and incorporate oxygen-containing groups [46,62]. An increase in number of oxygen functionalities manifested in an increase of ΔE_p ($[Fe(CN)_6]^{3-/4-}$) $\geq$ 0.36 V (see Fig. S1(A)). Between the individual measurements, the O-BDD electrode was re-activated directly in the analysed solution by applying +2.4 V for 30 s.

(ii) BDD surface was manually pre-treated using a polishing kit (BASi, USA) consisting of Texmet/alumina pads and an aqueous slurry of alumina powder (0.05 μm particle size) at the beginning of the working day for several minutes [62] until stable ΔE_p ($[Fe(CN)_6]^{3-/4-}$) value $\leq$ 0.10 V was assessed (see Fig. S1(A)). To renew the surface between the voltammetric scans, BDD electrode was removed from the analysed solution, polished for ~30 s on alumina polishing suspension and subsequently thoroughly rinsed with ultra-pure water. BDD electrode subjected to polishing pre-treatment is denoted as p-BDD.

The instrumental parameters for DPV experiments in NVP solutions, i.e., pulse amplitude (A), pulse width (t) and potential step (E_s), were carefully optimized separately for O-BDD (pH 2.0) and p-BDD (pH 5.0 and pH 13.0). The selected optimal value for each parameter was as follows: A of 130 mV, t of 20 ms, E_s of 10 mV for O-BDD, A of 100 mV, t of 30 ms, E_s of 15 mV for p-BDD (in pH 5.0), and A of 120 mV, t of 20 ms, E_s of 10 mV for p-BDD (in pH 13.0). Prior to optimization, particularly for pH study reported in Section 3.2, the used DPV parameters were A of 60 mV, t of 50 ms, and E_s of 15 mV for both electrodes.

The pH measurements were carried out using a pH-metre with a combined glass electrode (HI5522, Hanna Instruments, The Netherlands).

2.3. Analytical performance

Using optimized DPV parameters, analytical curves were constructed from the average of four replicate measurements for each NVP standard solution and evaluated by the least square's linear regression method. The limit of detection (LOD) and limit of quantification (LOQ) were assessed as a threefold and a tenfold of the standard deviation of the peak currents (n = 10) of the lowest measurable concentration, respectively, and divided by the slope of corresponding concentration dependence.

The intra-day (n = 10) and inter-day (n = 5) repeatability of the measurements under optimal conditions with incorporated pre-treatment step was evaluated for two concentration levels of NVP (10 μM and 100 μM) and was expressed by the respective relative standard deviations (RSD).

2.4. Interference study

The selectivity of the developed DPV methods was tested by the addition of possible interfering compounds typically present in biological fluids including blood serum. The effect of a 500-fold excess of inorganic cations and anions (Na^+, K^+, Ca^{2+}, Mg^{2+}, Cl^-, HPO_4^{2-}) and sugars (glucose, sucrose) on the voltammetric response of 10 μM NVP was evaluated. Further, the influence of the most common, easily oxidizable interferents, i.e., ascorbic acid, uric acid and dopamine, on the NVP signal (10 μM) was assessed at various concentration ratios of analyte to interferent (typically 1:1, 1:10, 1:25, 1:50, and 1:100). The interference was considered insignificant if the NVP signal intensity was altered less than ± 10%, compared to the peak current intensity recorded in the absence of the interfering compound.

2.5. Analysis of synthetic human serum

The applicability of the proposed methods was verified in the more complex matrix, specifically synthetic human serum, which was prepared according to the procedure proposed in [64]: 1.3 g of NaCl (87 mM), 0.16 g of $NaHCO_3$ (7.9 mM), 29 mg of aspartic acid (0.88 mM), 9.1 mg of alanine (0.41 mM), 10 mg of arginine (0.21 mM), 9.1 mg of lysine (0.20 mM), 6.6 mg of phenylalanine (0.16 mM), 2.3 mg of glycine (0.14 mM), 3.2 mg of serine (0.12 mM), 6.3 mg of histidine (0.12 mM), 3.7 mg of tyrosine (81 μM), and 3.5 mg of tryptophan (69 μM) were dissolved in deionized water in a 250 mL volumetric flask.

Prior to measurements, the synthetic serum was spiked with 50 μM NVP and subsequently diluted in a ratio of 1:1, 1:4, and 1:9 with the selected supporting electrolyte, thus the analysed spiked serum contained 25 μM, 10 μM, and 5 μM NVP, respectively. The standard addition method, utilising three aliquots of NVP stock solution (100 μL, 1 mM), was employed to assess the NVP concentration in the synthetic serum samples to eliminate the matrix effects.

3. Results and discussion

3.1. Effect of BDD surface termination

First, the effect of different surface pre-treatment of the BDD electrode was examined. To monitor the change in surface termination, CVs of two redox markers, $[Fe(CN)_6]^{3-/4-}$ and $[Ru(NH_3)_6]^{3+/2+}$ (both 1 mM in 1 M KCl), were recorded after anodic oxidation and then after polishing the BDD surface on alumina slurry (see Fig. S1). Subsequently, the ΔE_p values, indicating the rate of the HET kinetics, were extracted from the CV measurements.

The HET between the $[Fe(CN)_6]^{3-/4-}$ redox probe and the BDD electrode is of an inner-sphere nature and proceeds through specific surface interactions, hence HET is largely affected by the BDD surface properties, and particularly by the surface termination [48,51,54]. Subjecting the BDD electrode to anodic oxidation resulted in an increase in ΔE_p value ($\geq$ 0.36 V) indicating slower HET kinetics for $[Fe(CN)_6]^{3-/4-}$ marker. The inhibition of the electron transfer is caused by the presence of the oxygen-containing functionalities introduced on the BDD surface during anodic oxidation. Several works reporting XPS analysis have confirmed the formation of C-OH, C-O-C, C=O and even highly oxidized COOH and polycarbonate groups on the BDD surface [62,65] as a result of anodic treatment performed under conditions similar to the ones used in this study. Oxygen groups may either block the adsorption sites [54] for $[Fe(CN)_6]^{3-/4-}$ and/or electrostatically repel the anionic redox probe as they possess negative dipole moments ($-C^{\delta+}-O^{\delta-}$) [66]. However, when BDD surface was mechanically polished on alumina slurry, a considerable decrease in the ΔE_p value ($\leq$ 0.10 V) was found, as also documented in Fig. S1(A). This suggests faster HET kinetics for $[Fe(CN)_6]^{3-/4-}$ redox probe presumably due to the considerable reduction of the amount of oxygen functionalities. XPS spectra recorded for alumina-polished BDD surface in [62] were dominated by the sp^3 C-C peak and only small intensity peaks corresponding to C-OH, C-O-C and C=O groups were detected, while more heavily oxidized forms of carbon such as carboxyl and polycarbonate groups were completely absent. Assumedly, the remaining oxygen groups are not of sufficient quantity to inhibit HET kinetics of a surface-sensitive redox system.

The second utilised redox marker, $[Ru(NH_3)_6]^{3+/2+}$, exhibits outer-sphere character and its redox reaction is governed by simple diffusion, thus the HET rate is not affected by the BDD surface termination [54,66]. As expected, ΔE_p values recorded for the $[Ru(NH_3)_6]^{3+/2+}$

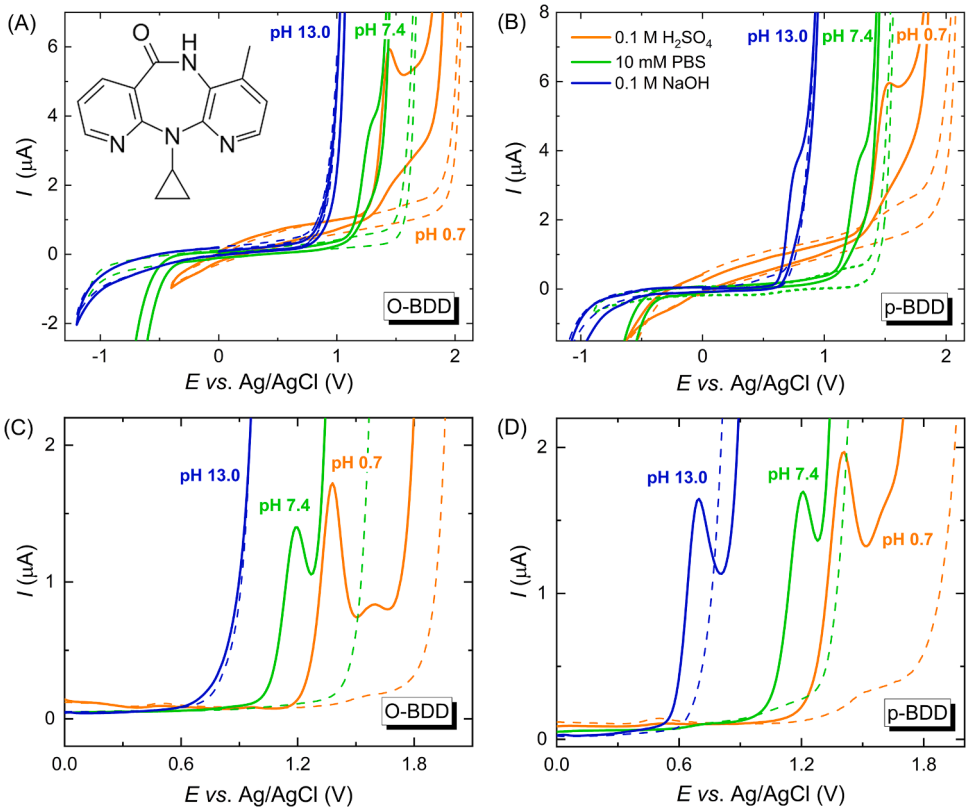

Fig. 1. (A, B) CVs and (C, D) DP voltammograms of 100 μM NVP recorded on (A, C) O-BDD and (B, D) p-BDD electrodes in (—— 0.1 M H_2SO_4 (pH 0.7), (——) 0.01 M PBS (pH 7.4), and (——) 0.1 M NaOH (pH 13.0). Dashed lines correspond to the supporting electrolyte. Inset in (A) displays the chemical structure of NVP.

redox marker (0.069 V and 0.079 V on O-BDD and p-BDD, respectively) remained nearly unchanged (see also Fig. S1(B)); these values even approach 0.059 V for a reversible redox reaction involving single-electron transfer. Further, the quasi-reversible character of $[Ru(NH_3)_6]^{3+/2+}$ was manifested when the scan rate study was performed and highly stable ΔE_p values of 0.071 ± 0.002 V on the O-BDD electrode and ΔE_p of 0.080 ± 0.003 V on the p-BDD electrode were acquired for the whole studied scan rate range, i.e., from 0.010 V s^{-1} to 0.250 V s^{-1} (see Fig. S1(C, D)). In the case of irreversible reactions, ΔE_p increases with an increase in scan rate. Moreover, linear dependences of anodic and cathodic peak currents (I_p) on the square root of the scan rate ($v^{1/2}$) (see the insets in Fig. S1(C, D)) and the slopes of log I_p vs. log v dependences ranging between 0.45 and 0.47 clearly demonstrate diffusion-controlled redox reaction of $[Ru(NH_3)_6]^{3+/2+}$ on both BDD electrodes. Besides, another parameter, particularly the effective surface area, A_{eff}, of the utilised BDD electrodes, was extracted from the scan rate measurements using the Randles-Sevcik equation (Eq. (1)) for a reversible process:

$$I_p = 2.69 \times 10^5 \; n^{3/2} \; A_{eff} \; D^{1/2} \; v^{1/2} \; c^0 \qquad \text{(Eq. 1)}$$

where n is the number of exchanged electrons (i.e., 1), D is the diffusion coefficient of $[Ru(NH_3)_6]^{3+/2+}$ (7.7×10^{-6} cm^2 s^{-1} [67]) and c^0 its concentration (10^{-6} mol cm^{-3}). For both O-BDD and p-BDD, A_{eff} of 5.4 mm^2 was calculated, which is smaller by 24% compared to A_{geom} (7.1 mm^2). This is, however, in accordance with previous works on BDD electrodes [50] with surfaces having heterogeneous character consisting of non-conductive (insulating) diamond matrix and boron-rich conductive (electroactive) sites [68,69].

Further, electrochemical behaviour of 100 μM NVP (structure depicted in Fig. 1) was investigated on the O-BDD and p-BDD electrodes by CV and DPV. The measurements were performed in three different environments of varying pH, particularly 0.1 M H_2SO_4 (acidic medium of pH 0.7), 0.01 M PBS (neutral medium of pH 7.4), and 0.1 M NaOH (alkaline medium of pH 13.0); the obtained voltammetric curves are depicted in Fig. 1.

CVs were recorded within the potential window available in the selected supporting electrolyte. As can be seen in Fig. 1 (A, B), NVP provided one oxidation peak on both electrodes in acidic and neutral electrolytes at the potential values of +1.45 V (O-BDD) and +1.53 V (p-BDD), and +1.29 V (O-BDD) and +1.27 V (p-BDD), respectively. The most pronounced difference between both surface terminations was recognized in a sodium hydroxide solution (pH 13.0) as NVP provided a detectable voltammetric signal only on the polished BDD surface. Moreover, no cathodic peak was detected in CVs recorded on O-BDD and p-BDD electrodes, which implied irreversible oxidation mechanism of NVP on this type of electrode material.

In the previous electrochemical studies on NVP drug, an alkaline medium (pH 8.0 – 12.0) was the most commonly employed in which NVP oxidized in the potential range from +0.67 V to +0.85 V on bare sp^2-carbon-based electrode materials (such as glassy carbon [26,28,29], carbon paste [24,27] and graphite electrode [25]). These values are comparable to the NVP oxidation on the p-BDD in a pH 13.0 environment occurring at a potential of +0.76 V.

Further, the same set of experiments was performed with the more sensitive DPV technique. The DPV curves were recorded in the potential range from 0 V up to the anodic limit of the potential window in a selected supporting electrolyte and are displayed in Fig. 1(C, D). On the polished surface (Fig. 1(D)), one anodic peak developed in all three media at a potential value of +1.41 V (H_2SO_4), +1.21 V (PBS), and +0.70 V (NaOH), while on the O-BDD electrode (Fig. 1(C)), no peak was recognized in alkaline medium in accordance with the CV measurements. Interestingly, two peaks at the potential values of +1.38 V and +1.60 V were recorded on the oxidized BDD surface in acidic medium (pH 0.7) and one peak at a lower value of +1.19 V was developed in a pH 7.4 buffer.

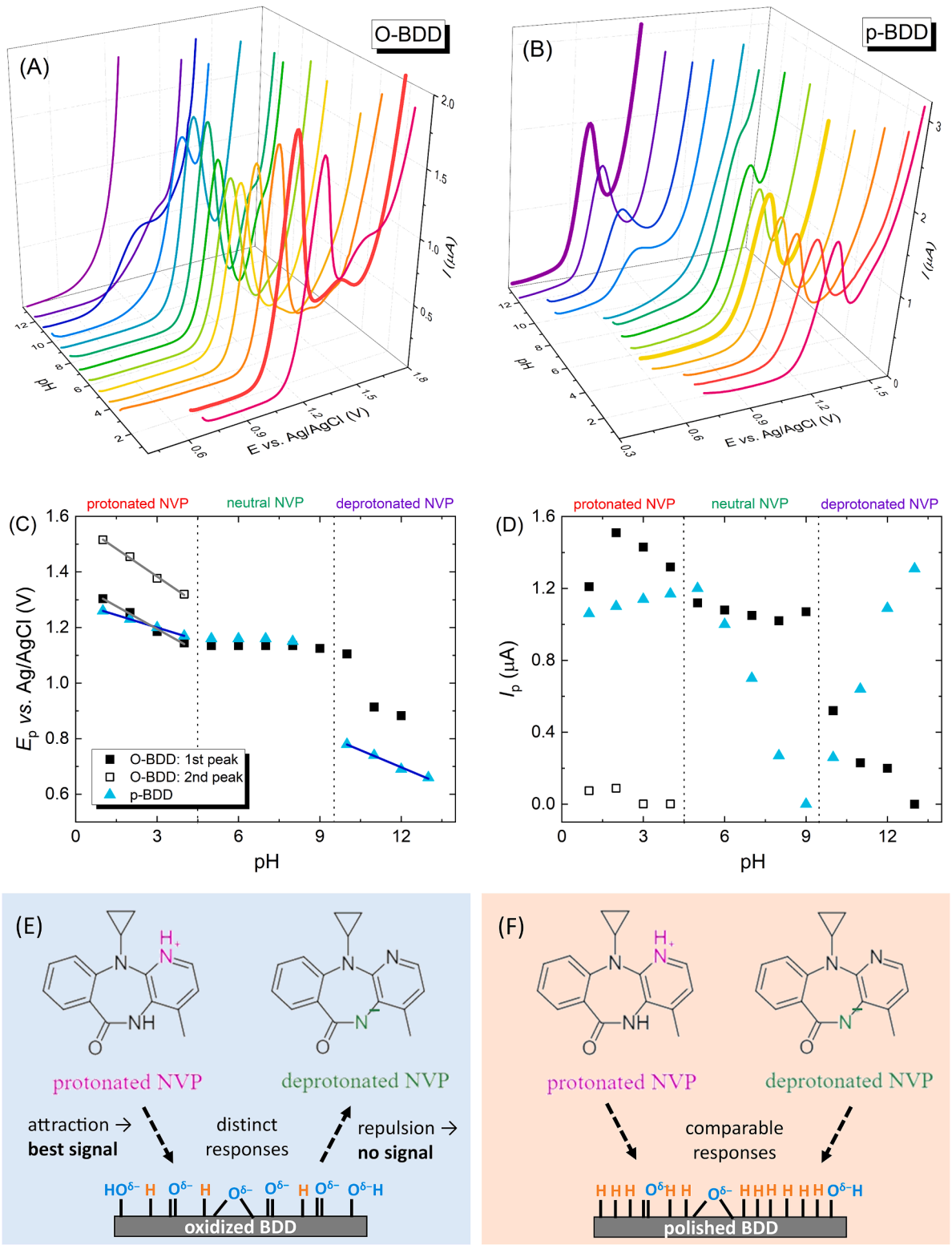

Fig. 2. DP voltammograms of 100 μM NVP in the solutions with pH ranging between 1.0 and 13.0 recorded on (A) O-BDD electrode and (B) p-BDD electrode. The dependences of (C) peak potentials E_p on pH (with linear fits indicated in acidic and alkaline pH regions) and (D) peak currents I_p on pH obtained for (■■) O-BDD and (●) p-BDD electrodes. Simplified schematics depicting interactions of ionized NVP forms with (E) O-BDD and (F) p-BDD surfaces.

Briefly, the electrochemical behaviour of NVP is influenced (i) by the supporting electrolyte and its pH and (ii) the state of the BDD surface (oxidized vs. polished).

3.2. *Effect of pH and supporting electrolyte*

To further clarify the effect of pH and surface pre-treatment, a thorough pH study was performed with 100 μM NVP in BR buffers of pH 2.0 – 12.0 (with a step of pH 1.0), 0.1 M HCl (pH 1.0) and 0.1 M NaOH

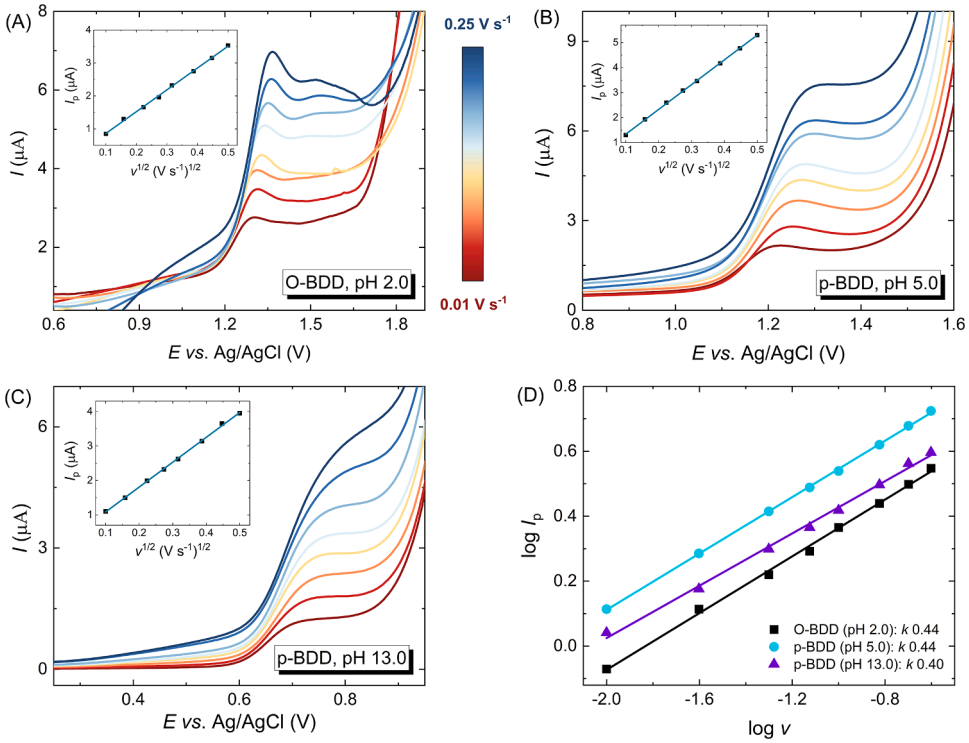

Fig. 3. LS voltammograms of 100 μM NVP for the range of scan rates v on (A) O-BDD in 0.04 M BR buffer (pH 2.0), (B) p-BDD in 0.1 M acetic buffer (pH 5.0), and (C) p-BDD in 0.1 M NaOH (pH 13.0). Insets in (A–C) display linear dependence of NVP peak currents (I_p) on the square root of the scan rate ($v^{1/2}$). (D) Dependences of log I_p vs. log v along with the slope values acquired from the scan rate studies.

(pH 13.0) on O-BDD and p-BDD electrodes. Obtained DPV curves are displayed in Fig. 2 (A, B) and show the marked differences between the examined BDD surfaces manifested by the number of NVP voltammetric signals, their potentials and intensities; while these are also strongly dependant on pH of the supporting electrolyte, as clearly demonstrated by Fig. 2 (C, D).

In acidic media of pH 1.0 – 4.0, NVP provides two anodic peaks on the oxidized BDD surface, while only one peak appears in the DP voltammograms recorded on the polished electrode. However, a common feature recognized for both electrodes is a linear shift of NVP peak potentials (E_p) towards lower values with an increase in pH from 1.0 to 4.0, which can be expressed by the following equations (Eqs. (2)–(4)):

$$\mathrm{O-BDD}: E_{p,1}(\mathrm{V}) = (-0.055 \pm 0.003)\mathrm{pH} + (1.36 \pm 0.01) \qquad R = 0.994 \qquad \text{(Eq. 2)}$$

$$\mathrm{O-BDD}: E_{p,2}(\mathrm{V}) = (-0.067 \pm 0.003)\mathrm{pH} + (1.58 \pm 0.01) \qquad R = 0.997 \qquad \text{(Eq. 3)}$$

$$\mathrm{p-BDD}: E_{p}(\mathrm{V}) = -0.030\mathrm{pH} + 1.29 \qquad R = 1 \qquad \text{(Eq. 4)}$$

The slopes of −0.055 V/pH and −0.067 V/pH for the first and second oxidation peak, respectively, acquired on the O-BDD electrode approach the theoretical Nernstian slope of −0.059 V/pH, and thus indicate that the redox reaction of NVP (and its oxidation product) comprises of equal number of protons and electrons. In contrast, the slope of −0.030 V/pH assessed on p-BDD suggests the oxidation mechanism involving unequal number of protons and electrons.

A linear shift limited to pH 4.0 is presumably associated with the value of strongest basic pK_a of NVP, i.e., pK_a of its protonated form, being 3.28 [70]. Until ca pH 4.3, fractions of both protonated and neutral NVP molecules are present in the solution, while at pH ≥ 4.3, vast majority of NVP molecules exist only in neutral form. Indeed, a change in behaviour of NVP was detected at pH 5.0 as practically stable peak potential values were recorded for NVP oxidation in the range of pH 5.0 – 10.0 and pH 5.0 – 8.0 on the O-BDD and p-BDD electrodes, respectively (see Fig. 2(C)). According to [70], more than 90% of NVP molecules are uncharged in the pH range of 5.0 – 9.0. Similar observation on pH independence for neutral forms of structurally close nitrogen-based heterocyclic compounds on the BDD electrode was reported in [41]. However, at pH ≥ 9.0, dissociation of NVP starts to occur which is related to the strongest acidic pK_a of NVP, i.e., pK_a of the dissociated form, being 9.98 [70]. In alkaline media (pH 10.0 – 13.0), again a linear shift in NVP peak potential (E_p) towards lower values with an increase in pH could be recognized on the polished BDD surface, and this shift can be expressed by the equation (Eq. (5)):

$$E_p(\mathrm{V}) = (-0.041 \pm 0.003)\mathrm{pH} + (1.19 \pm 0.03) \qquad R = 0.994 \qquad \text{(Eq. 5)}$$

The slope of −0.041 V/pH proposes participation of unequal number of protons and electrons in the NVP oxidation in alkaline media on the p-BDD electrode. In contrast, a considerable decrease by 0.19 V in the peak potential was noticed on the O-BDD electrode between pH 10.0 and 11.0 and NVP signals of only small intensity ($I_p \sim 200 – 230$ nA) were noticed in pH 11.0 and 12.0, while no NVP peak developed in a pH 13.0 medium. This can be explained by the fact that NVP molecules are fully dissociated (negatively charged), and hence repelled from the oxidized BDD surface containing negatively charged oxygen groups, as schematically proposed in Fig. 2(E).

On the contrary, in acidic media NVP occurs predominantly in its protonated (positively charged) form and is thus attracted to the oxygen-terminated BDD surface (see Fig. 2(E)). Consequently, the highest peak intensity for NVP on O-BDD was achieved in a pH 2.0 buffer, as Fig. 2(D) clearly shows, hence the pH value of 2.0 was recognized as the most appropriate for NVP study on the oxidized BDD surface. With a further increase in pH, NVP peak currents gradually decrease (see Fig. 2(D)).

The electrostatic interactions played an essential role also in previously reported works involving NVP, e.g., in [25] the enhancement in the NVP peak current at pH > 10 was ascribed to the fact that dissociated

NVP was attracted to positively charged poly(methylene blue) used as one of the electrode modifiers. Similarly, protonated amide groups of a modifier at the electrode surface [26] and positively charged polymer used in the preparation of molecularly imprinted sensor [32] prevented NVP oxidation in acidic media, where NVP is also protonated (positively charged). Moreover, repulsion from negatively charged O-BDD has been recognized as a main factor responsible for the degraded electrochemical responses of compounds with dissociated carboxylic moieties (-COO^-) in neutral and/or alkaline media [38,55] and compounds possessing phosphate functional groups such as adenosine di-/tri-phosphates [39].

As Fig. 2(D) suggests, several trends can be identified on the p-BDD; the intensity of NVP peak (i) increases slightly from pH 1.0 to 5.0, (ii) then continuously decreases until pH 9.0, and (iii) finally steadily increases up to pH 13.0. In contrast to O-BDD, comparable peak intensities were recorded on p-BDD for both protonated (pH < 4.0) and fully deprotonated (pH 12.0 and 13.0) forms of NVP, indicating that on polished surface, with much smaller oxygen content, NVP responses are not affected by the electrostatic interactions (as depicted in Fig. 3(F)). Overall, strongest NVP signals were developed in pH 5.0 and pH 13.0 environments, which were selected for further voltammetric experiments with NVP on the polished BDD electrode.

With the most suitable pH values identified, the effect of type of supporting electrolyte on the NVP signals (100 μM) was examined. On the O-BDD electrode, comparable NVP voltammetric responses were recorded in three media of pH 2.0: 0.04 M BR buffer, 0.1 M phosphate buffer, and 0.01 M HCl + 0.1 M KCl solution, however, slightly higher peak currents were recognized in BR buffer, which was thus selected as optimal environment for further NVP study on the oxidized BDD. In case of p-BDD electrode, also three media of pH 5.0 were tested and compared, specifically 0.04 M BR buffer, acetic and citric buffers (both 0.1 M), and the NVP signals of the highest intensities were recognized in acetic buffer, consequently chosen as the most suitable representative of pH 5.0 media. For pH 13.0 environment, 0.1 M NaOH was preserved as a strongly alkaline electrolyte.

3.3. Scan rate study

To clarify the nature of the electrochemical oxidation of NVP on the O- and p-BDD electrodes, a scan rate study, using LSV, was carried out. Fig. 3 depicts the LS voltammograms of 100 μM NVP recorded at scan rates ranging from 0.010 V s^{-1} up to 0.250 V s^{-1}. Notably, only one peak associated with NVP oxidation was recorded at slower scan rates (up to 0.10 V s^{-1}) on the O-BDD electrode, while two peaks could be clearly distinguished when LSV curves were recorded using higher scan rates.

LS voltammetric currents (I_p) increased linearly with an increase in the square root of the scan rate ($\nu^{1/2}$); the linear dependences for each electrode and medium are shown as insets in Fig. 3 and the corresponding equations are stated in the Supplementary material. The linear I_p vs. $\nu^{1/2}$ dependences proved that the NVP oxidation on the O-BDD and p-BDD electrode surfaces is governed by diffusion. This claim can be further supported by log I_p vs. log ν analysis, shown in Fig. 3(D), for which the slopes in the range of 0.40 – 0.44 were extracted. These slope values are very close to the theoretical value of 0.50 for diffusion-controlled processes (when the slope approaches 1.0, the redox process is adsorption-confined). The complete equations can be found in the Supplementary material.

Besides, a shift in the NVP peak potential towards more positive values with the increasing scan rate was recognized on the O-BDD and p-BDD electrodes in all three media, which further confirms the irreversible voltammetric behaviour of the studied anti-HIV drug, as already suggested in Section 3.1. The dependences of NVP peak potential (E_p) on the logarithm of the scan rate (log ν) were found linear (Eqs. (6)–(8)):

$$\mathrm{O-BDD(pH2.0)}: E_p(\mathrm{V}) = (0.061 \pm 0.003)\log\nu + (1.403 \pm 0.004),\ R = 0.991 \quad \text{(Eq. 6)}$$

$$\mathrm{p-BDD(pH5.0)}: E_p(\mathrm{V}) = (0.058 \pm 0.001)\log\nu + (1.336 \pm 0.001),\ R = 0.999 \quad \text{(Eq. 7)}$$

$$\mathrm{p-BDD(pH13.0)}: E_p(\mathrm{V}) = (0.058 \pm 0.002)\log\nu + (0.836 \pm 0.003),\ R = 0.999 \quad \text{(Eq. 8)}$$

Next, the Laviron's equation (Eq. (9)) proposed for irreversible oxidation processes [71] was employed to obtain information on the number of transferred electrons (n):

$$E_p = E^0 + \left(\frac{2.303RT}{nF}\right)\log\left(\frac{RTk^0}{nF}\right) + \left(\frac{2.303RT}{\alpha nF}\right)\log\nu \quad \text{(Eq. 9)}$$

where E^0 is the formal standard redox potential, k^0 is the heterogeneous rate constant, ν is the scan rate, T is thermodynamic temperature (296.15 K), and R and F are gas (8.314 J K^{-1} mol^{-1}) and Faraday (96 485 C mol^{-1}) constants, respectively.

Using the slopes of Eqs. (6)–(8) and considering α = 0.5 (for an irreversible redox reaction), the number of electrons (n) involved in the rate-determining step of NVP oxidation was evaluated to be 1.91 (i.e., 2 electrons) on the O-BDD electrode in a pH 2.0 buffer and to be 2.03 (i.e., 2 electrons) on the p-BDD electrode in both pH 5.0 and pH 13.0 electrolytes.

In addition, the E^0 values were simply estimated as the intercepts of the plots of E_p vs. ν (extrapolated for $\nu = 0$) [35] as follows: +1.27 V on O-BDD electrode (pH 2.0 buffer), +1.21 V on p-BDD (pH 5.0 buffer), and +0.71 V on p-BDD (in NaOH solution, pH 13.0).

Based on the electrochemical results obtained and the available relevant literature on NVP [22] and compounds with a similar structural moiety such as guanine [72], the mechanism of NVP electrooxidation on a BDD electrode was proposed and is depicted in Scheme 2 (for non-ionized NVP form in a medium of pH 5.0 – 9.0). The first step includes the attachment of a hydroxyl group and the transfer of two electrons, which correspond well with the above-mentioned estimation of two electrons involved in the rate-limiting step. Assumedly, the hydroxylated NVP oxidation product can isomerise into its keto-tautomer and may be further oxidized, which is accompanied by the loss of two other electrons. Thus, the overall NVP oxidation mechanism involves four electrons, while the number of protons may vary depending on the NVP form (protonated vs. neutral vs. dissociated).

3.4. Analytical performance

3.4.1. Optimization of DPV parameters

Since NVP oxidation on a bare BDD surface is of irreversible nature and governed by diffusion, DPV technique was favourably selected to develop sensitive, selective and reliable NVP determination procedure on the BDD electrodes with different surface characteristics (oxidized vs. polished) and in various environments. To this goal, key operational DPV parameters affecting the NVP signal intensity (peak current) as well as the shape of the voltammetric peak and its position (peak potential), specifically pulse amplitude (A), pulse width (t) and potential step (E_s), were carefully optimized. The optimization process was carried out in 100 μM NVP solutions separately for O-BDD (in a pH 2.0 buffer) and p-BDD electrode (in pH 5.0 and 13.0 media). The effect of each parameter on the analytical signal of NVP was tested in the following ranges: A 10 – 200 mV, t 10 – 70 ms, and E_s 5 – 25 mV, and whilst investigated parameter varied, the other two were kept constant. The final optimal parameters selected as a trade-off between the intensity and the shape of the NVP peak are as follows: (i) O-BDD (in pH 2.0): A 130 mV, t 20 ms, E_s 10 mV; (ii) p-BDD (in pH 5.0): A 100 mV, t 30 ms, E_s 15 mV; (iii) p-BDD (in pH 13.0): A 120 mV, t 20 ms, E_s 10 mV.

3.4.2. Stability of the NVP voltammetric responses

Several sets of experiments were carried out under optimized conditions, i.e., supporting electrolyte and DPV parameters, to investigate

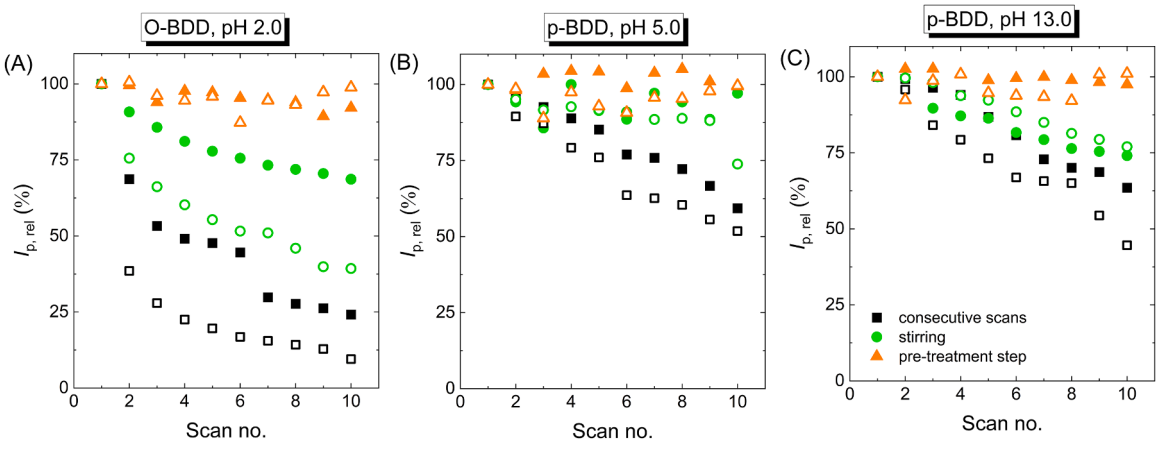

Fig. 4. Relative peak heights ($I_{p,rel}$) of 10 μM NVP (full symbols) and 100 μM NVP (open symbols) recorded on (A) O-BDD electrode in 0.04 M BR buffer of pH 2.0, (B) p-BDD electrode in 0.1 M acetic buffer of pH 5.0, and (C) p-BDD electrode in 0.1 M NaOH (pH 13.0). Ten DPV scans were acquired (■■) consecutively, (●○) with the stirred analysed solution between the individual measurements, and (▲△) with the pre-treatment step included between the scans, either 30 s of anodic oxidation on O-BDD or 30 s of polishing on p-BDD electrode.

the stability of NVP signals. For two NVP concentration levels, 10 μM and 100 μM, ten DPV scans were recorded (i) consecutively without any pre-treatment step nor stirring, (ii) with stirring the analysed solution, and (iii) with the incorporated pre-treatment step, i.e., 30 s of anodic activation on O-BDD or 30 s of polishing on p-BDD. Both peak potentials and peak currents of NVP signals were assessed, and while potential values remained practically stable (with a change of maximum ± 0.010 V), peak currents altered depending on the measurement conditions, as shown in Fig. 4 and Table S1.

In the first set of measurements, with the DPV curves recorded successively, a continuous decrease in NVP voltammetric responses was recognized on O-BDD and p-BDD electrodes in all media. This is caused by a combination of two main factors: a decrease in a local NVP concentration close to the BDD surfaces, which are simultaneously fouled by the oxidation product(s). Nevertheless, much more pronounced drop in peak intensity was observed on the O-BDD electrode, compared to the electrode with polished surface as shown in Fig. 4. On anodically oxidized BDD, the difference between the first and second scan represented 61.5%, while after ten measurements, a 87.2% decrease was recognized for more concentrated 100 μM NVP solution. In contrast, NVP peak currents lowered after ten scans approximately by a third or by a half on the p-BDD electrode in pH 5.0 and pH 13.0 media, respectively. This could be due to the different properties of O-BDD and p-BDD electrodes; the latter is electrode type more hydrophobic with smaller oxygen content, which makes it less prone towards fouling by the oxidation products with hydrophilic carbonyl groups (see Scheme 2). Presumably, such reaction products have higher affinity towards oxygenated BDD surface and electrode passivation occurs predominantly via hydrophilic interactions. In previous works, carbon-based surfaces with lower amount of polar (oxygen-containing) groups indeed showed higher resistance to electrode bio(fouling) [56,73].

When the NVP solution was simply stirred between each measurement, a decrease in NVP peak currents was suppressed as a contribution of a decline in local NVP concentration was eliminated because stirring restored the bulk NVP concentration also in a proximity to the BDD surfaces, while the effect of fouling could also be partially inhibited. As Fig. 4 indicates, a gradual decrease in peak currents occurred in a smaller extent; the only exception was 10 μM NVP in acetic buffer of pH 5.0 in which rather stable responses were acquired with RSD of 5.3%.

Notably, incorporation of a respective pre-treatment step ensured highly repeatable NVP signals on both O-BDD and p-BDD electrodes in all three media, leading to excellent intra-day repeatability ($n = 10$) with RSD of less than 4% (see Table S1). Further, inter-day repeatability (RSD, $n = 5$), evaluated for NVP concentrations of 10 μM and 100 μM, was correspondingly 2.8% and 1.9%, 4.0% and 1.9%, and 3.6% and 6.5% on O-BDD in BR buffer of pH 2.0, p-BDD in acetic buffer of pH 5.0 and p-BDD in NaOH solution (pH 13.0). The values acquired for intra- and inter-day repeatability confirm excellent stability of the NVP voltammetric responses when a simple and quick pre-treatment step is included and highlight reliability of the BDD surface for NVP detection. Another advantage is that the BDD electrode is applied in a convenient modification-free condition, hence if necessary, the electrode surface can be easily re-activated by the prolonged exposure to the pre-treatment procedures without a need to repeat the multi-step and tedious modification processes proposed previously for sp^2-carbon-based electrodes (e.g., see [22,26,29,30]). Besides, modified electrode surfaces typically suffer more from signal instability and fabrication irreproducibility.

3.4.3. *Concentration dependences*

Next, the concentration dependences of the anti-HIV agent NVP were recorded under optimized conditions on O-BDD and p-BDD electrodes; the obtained DP voltammograms are depicted in Fig. 5. The acquired analytical parameters, including linear range and sensitivity, and calculated LOD and LOQ values are summarized in Table 1.

Fig. 5 shows that the oxidation peak currents increased with an increase in NVP concentration. Only one linear range was observed on p-BDD electrode in both environments, while three ranges can be identified for the O-BDD electrode, on which also submicromolar NVP concentrations could be recorded. Similarly, two or three linear ranges were recognized in several previous electroanalytical studies on NVP [22,25,33].

In general, O-BDD electrode outperformed p-BDD electrode in terms of sensitivity and the lowest detection limit achieved (40 nM). However, it needs to be emphasized that both electrodes in all three media provided highly satisfactory parameters (see Table 1) which fulfil the requirements for their practical, possibly clinical, application for NVP sensing and monitoring in biofluids such as blood plasma and serum. In practice, after 4 h since oral administration of a single 200 mg NVP tablet, a peak plasma concentration of 7.5 ± 1.5 μM is reached [2,20], while steady-state through concentration of NVP in blood plasma during the long-term treatment (400 mg NVP / day) is in a range of 17 ± 7 μM [2]. Such concentration values fit perfectly in the recorded concentration dependences of NVP on the BDD electrodes, which showed highly satisfactory LOD values as well.

Table S2 in Supplementary material provides an overview of electroanalytical methods developed for NVP determination. The non-modified BDD electrodes certainly compete very well with the

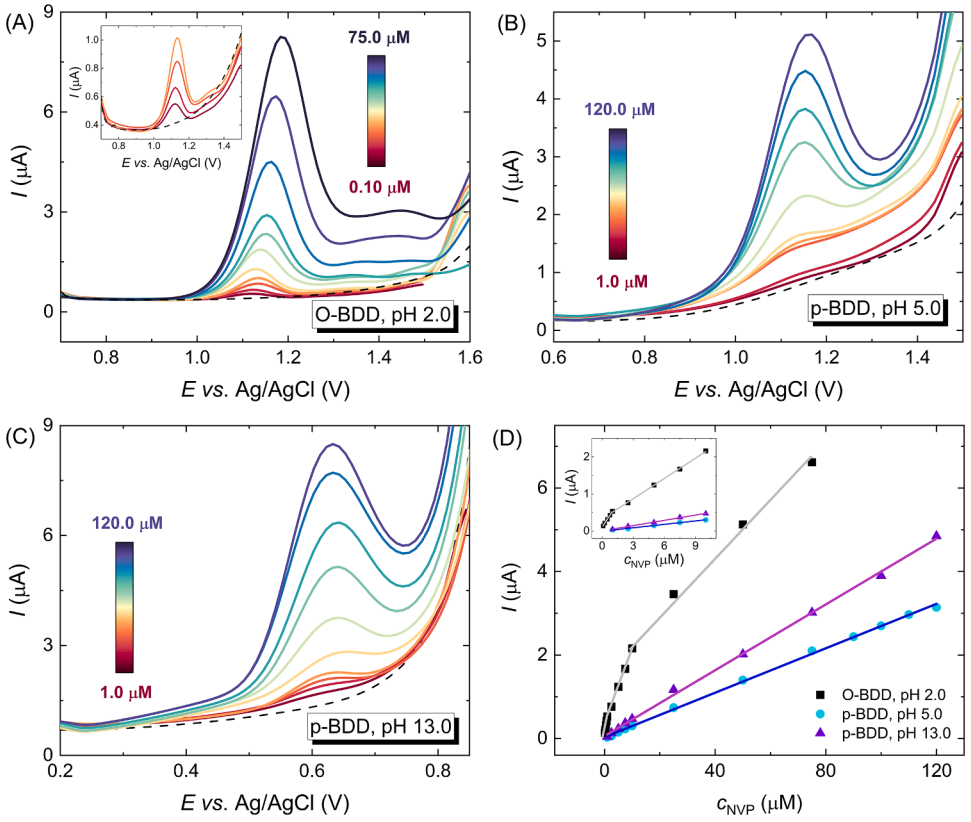

Fig. 5. DP voltammograms of NVP at different concentration levels recorded on (A) O-BDD electrode in 0.04 M BR buffer of pH 2.0 (inset displays a detail of voltammograms recorded for the lowest concentrations), (B) p-BDD electrode in 0.1 M acetic buffer of pH 5.0, and (C) p-BDD electrode in 0.1 M NaOH (pH 13.0). Dashed lines correspond to the supporting electrolyte. (D) Concentration dependences of NVP recorded by the developed DPV methods on the respective BDD electrodes. Inset shows detail for lower concentration values (from 0.1 μM up to 10 μM).

Table 1
Analytical parameters of NVP concentration dependences recorded by developed DPV methods using anodically oxidized (O-) and polished (p-) BDD electrode.

Electrode	Electrolyte	Linear range (μM)	Intercept $\times 10^{-2}$ (μA cm^{-2})	Slope $\times 10^{-2}$ (μA μM^{-1} cm^{-2})	R	LOD (μM)	LOQ (μM)
O-BDD	0.04 M BR buffer, pH 2.0	0.10 – 1.0	−9.75 ± 0.39	43.44 ± 0.63	0.9996	0.04	0.12
		1.0 – 10.0	32.76 ± 1.85	18.17 ± 0.30	0.9994		
		10.0 – 75.0	162.74 ± 16.63	6.79 ± 0.35	0.9959		
p-BDD	0.1 M acetic buffer, pH 5.0	1.0 – 120.0	3.33 ± 1.85	2.66 ± 0.03	0.9994	0.30	1.00
p-BDD	0.1 M NaOH, pH 13.0	1.0 – 120.0	6.01 ± 2.84	3.94 ± 0.05	0.9993	0.27	0.90

electrodes utilised in the previous works, which had to often undergo complicated and tedious modification procedure to achieve the same or slightly improved analytical parameters. Moreover, a considerable portion of previously reported methods [22,24,25,27,32,33] employ accumulation steps of tens of seconds which naturally prolong the analysis time.

3.5. Interference study

Further, the selectivity of the proposed DPV methods for NVP detection was examined. The voltammetric response of 10 μM NVP recorded on the BDD electrodes was evaluated in the absence and the presence of common interfering compounds at various concentration levels (details are listed in Section 2.4); Fig. S2 in Supplementary material shows selected DP voltammograms recorded with interferents present in the analysed NVP solutions.

Fig. 6 provides an overview of to what extent the NVP peak current was influenced by the addition of an interfering compound of a certain concentration. Clearly, NVP signals remain basically unaffected by an addition of a 500-fold of inorganic salts and carbohydrates (glucose and sucrose) in all three media on O-BDD and p-BDD electrode. Dopamine occurs in plasma typically at very low concentrations ($\leq$ 0.1 μM) and it was proved that even much larger dopamine concentrations of 50 μM (O-BDD) and 100 μM (p-BDD) do not cause any interference with NVP determination. In contrast, concentration of other two tested electroactive interferents present in blood plasma, namely ascorbic acid and uric acid, ranges correspondingly from 10 μM to 115 μM [74] and from 150 μM to 550 μM (depending on the gender) [75]. As indicated by Fig. 6, physiological levels of ascorbic acid do not affect NVP signals obtained on p-BDD electrodes (in pH 5.0 and pH 13.0 environments). However, on the O-BDD electrode in a pH 2.0 medium, the proximity of oxidation potentials of ascorbic acid (+1.06 V) and NVP (+1.15 V) causes an overlay of their peaks at higher ascorbic acid concentrations ($\geq$ 50 μM), which subsequently causes an increase in NVP voltammetric response (more than tolerated ± 10% change). Further, due to the limited solubility of uric acid in acidic media of pH 2.0 (O-BDD) and pH 5.0 (p-BDD), the maximal tested uric acid concentration was 250 μM. Even at this level, no interfering effect on the NVP signal was recognized. On the contrary, uric acid is well soluble in alkaline medium (0.1 M NaOH, pH 13.0). The concentrations of uric acid higher than 100 μM disturbs the NVP drug determination because the peaks of the two compounds partially overlap, which decreases the intensity of NVP signals.

Nevertheless, it should be noted that electroanalysis in human plasma and serum requires prior sample treatment and processing including dilution with a selected supporting electrolyte (to adjust pH to

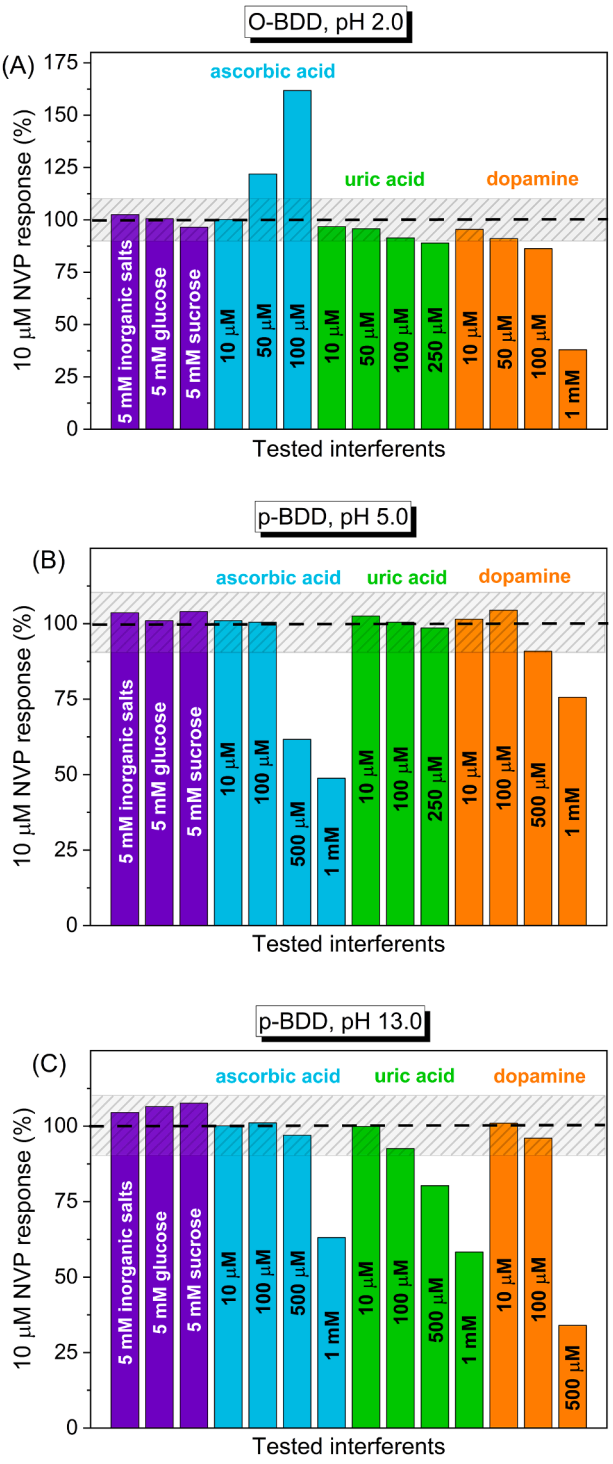

Fig. 6. Relative DP voltammetric response of 10 µM NVP acquired in the presence of several interfering compounds at different concentration levels on (A) O-BDD electrode in 0.04 M BR buffer of pH 2.0, (B) p-BDD electrode in 0.1 M acetic buffer of pH 5.0, and (C) p-BDD electrode in 0.1 M NaOH (pH 13.0). The dashed grey zones indicate the tolerated ± 10% alteration in the peak current intensities of NVP signals.

the optimized value), which naturally decreases concentration of the interfering compounds. Therefore, in such real sample analysis, no serious interfering effects of the ascorbic acid and uric acid are expected and reliable determination of NVP on the BDD electrodes can thus be successfully accomplished.

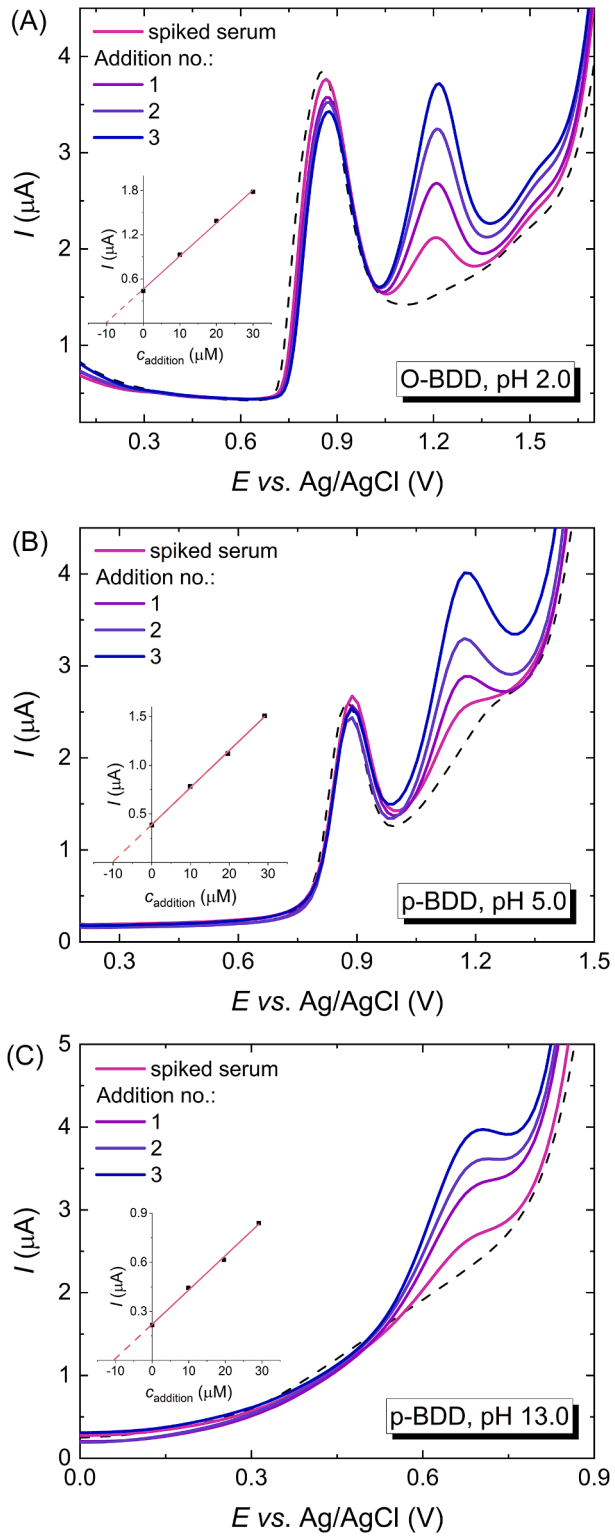

Fig. 7. DP voltammograms recorded in the synthetic serum samples diluted with the corresponding supporting electrolyte (1:4) and spiked with 10 µM NVP, followed by the three standard additions (all 100 µL, 1 mM NVP) on (A) O-BDD (pH 2.0), (B) p-BDD (pH 5.0), and (C) p-BDD (pH 13.0). Dashed lines correspond to the diluted synthetic serum sample without spiked NVP. Insets demonstrate the graphical quantification of NVP using a standard addition method.

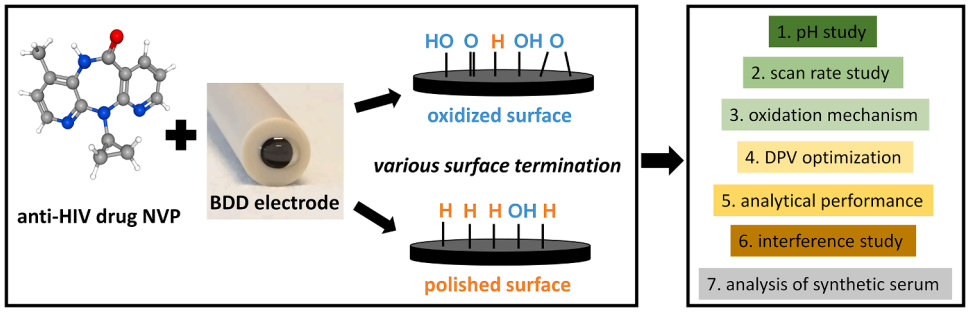

Scheme 1. Visualisation of the conducted work.

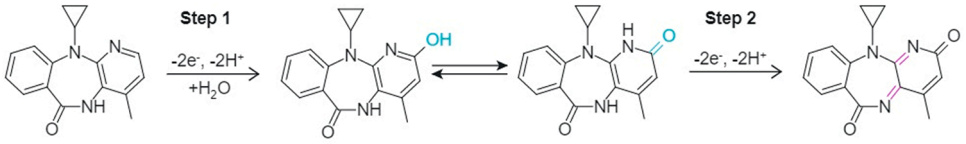

Scheme 2. Proposed mechanism of electrochemical oxidation of the anti-HIV agent NVP.

Table 2
Results acquired for NVP determination in synthetic serum samples ($n = 4$) using the standard addition method.

Electrode	Spiked (μM)	Found (μM) ± $L_{1,2}$ [a]	Recovery [b]
O-BDD (pH 2.0)	5.0	4.95 ± 0.18	99.0%
	10.0	9.81 ± 0.30	98.1%
	25.0	24.08 ± 0.81 [c]	96.3%
p-BDD (pH 5.0)	5.0	5.07 ± 0.16	99.2%
	10.0	10.53 ± 0.37 [c]	105.3%
	25.0	25.29 ± 1.07	101.2%
p-BDD (pH 13.0)	5.0	5.08 ± 0.11	101.6%
	10.0	9.87 ± 0.29	98.7%
	25.0	25.76 ± 0.87	103.0%

[a] Confidence interval calculated using equation: $L_{1,2} = (t_{n-1,\alpha} / \sqrt{n}) \times SD$ [21]; $t_{3,0.05} = 3.182$.
[b] Recovery (%) = (found concentration / spiked concentration) × 100.
[c] The spiked value is not covered by the interval but it is very closely approached.

Moreover, four hydroxyl metabolites (with –OH group at positions 2, 3, 8, and 12) and one 4-carboxy metabolite of NVP have been identified in patients' plasma samples [76]. These metabolites are likely electroactive, however, since their concentration is always significantly smaller (< 0.5 μM) [76] than the NVP plasma concentration (17 ± 7 μM), due to a long plasma half-life of NVP (25 – 30 h) [2], they are not expected to cause any serious interferences and to compromise selectivity of NVP detection.

3.6. Analysis of synthetic serum samples

Finally, the suitability of the proposed DPV methods for practical applications, e.g., monitoring and detection of NVP in relevant biological fluid (blood serum) was verified. O-BDD and p-BDD electrodes were employed to determine NVP in spiked synthetic human serum samples (prepared as described in Section 2.5).

In the synthetic serum diluted with pH 2.0 and pH 5.0 buffers, a high intensity peak appeared at a potential around +0.85 V (see Figs. 7 and S3). Electroactive and oxidizable amino acids, such as tyrosine and tryptophan, present in the synthetic serum are presumably responsible for the peak development. In strongly alkaline medium of 0.1 M NaOH (pH 13.0), no peak originating from the synthetic serum matrix was detected.

To suppress the matrix effects, standard addition method was selected to accurately determine NVP in the spiked serum samples, while physiologically relevant NVP concentration levels (5 μM, 10 μM, and 25 μM; see Section 3.4.3) were selected. The results obtained are summarized in Table 2 and the DP voltammograms recorded for the serum samples spiked with 10 μM NVP are displayed in Fig. 7 (for other two spiked values, see Fig. S3). In addition, Table 2 provides recovery values obtained from the electroanalysis of synthetic serum samples spiked with NVP using O-BDD and p-BDD electrodes. The values are in the highly satisfactory range of 96.3% – 103.0% and confirm that the DPV methods, utilising O-BDD as well as p-BDD, developed in this study for NVP sensing are suitable and applicable for practical clinical applications.

4. Conclusion

In the present work, a non-modified BDD electrode was successfully verified as an outstanding sensing tool toward reliable and sensitive detection of the antiretroviral agent NVP. The BDD electrode was subjected to two types of simple pre-treatment procedures to examine the effect of surface termination (high vs. low oxygen content) on the voltammetric behaviour of NVP. The compound exists in the aqueous solutions in several forms depending on the pH value, which is a crucial aspect influencing NVP voltammetric responses on a partially negatively charged O-BDD surface where electrostatic interactions play a significant role.

DPV methods developed for NVP detection provided highly favourable analytical figures of merit and satisfied practical requirements for NVP monitoring in clinical matrices, which was also successfully verified during electroanalysis of NVP in synthetic serum samples. Importantly, the outstanding features of the BDD electrode enabled developing a direct, simple, and rapid protocol for NVP detection, and thus the possibility to avoid complex and tedious modification procedures as well as accumulation steps was demonstrated.

Consequently, this work opens a path for the development of a complete sensing platform with integrated BDD, which can be applied to analysis not only in physiological fluids but also in environmental samples in which NVP occurs as a persistent contaminant. BDD is advantageously used for pollutants degradation and water treatment applications, therefore a device with an ability to first detect and subsequently to degrade NVP may be envisioned in the future. Nevertheless, it should be pointed out that in order to detect NVP in environmental samples where its concentration is typically at nM levels, a

modification of the BDD surface, either by employing surfactants allowing analyte pre-concentration or nanomodifiers having electrocatalytic effects, may be required.

CRediT authorship contribution statement

Simona Baluchová: Conceptualization, Investigation, Data curation, Formal analysis, Visualization, Writing – original draft, Writing – review & editing. **Antigoni Mamaloukou:** Investigation, Data curation, Formal analysis, Writing – review & editing. **Rombert H.J.M. Koldenhof:** Investigation, Writing – review & editing. **Josephus G. Buijnsters:** Conceptualization, Supervision, Writing – review & editing, Funding acquisition, Project administration.

Declaration of Competing Interest

The authors declare that they have no known competing financial interests or personal relationships that could have appeared to influence the work reported in this paper.

Data availability

Data will be made available on request.

Acknowledgements

Financial support from the Dutch Research Council (NWO) through the Open Technology Programme [project no. 16361] is gratefully acknowledged.

Supplementary materials

Supplementary material associated with this article can be found, in the online version, at doi:10.1016/j.electacta.2023.142238.

References

[1] A.M.N. Tsibris, M.S. Hirsch, J.E. Bennett, R. Dolin, M.J. Blaser, 130 - Antiretroviral therapy for human immunodeficiency virus infection. Mandell, Douglas, and Bennett's Principles and Practice of Infectious Diseases, 8th ed., W.B. Saunders, Philadelphia, 2015, pp. 1622–1641.

[2] Boehringer Ingelheim (Canada) Ltd, VIRAMUNE Product Monograph: Antiretroviral Agent Non-Nucleoside Reverse Transcriptase Inhibitor with Activity Against Human Immunodeficiency Virus Type 1 (HIV-1), Boehringer Ingelheim (Canada) Ltd, 2013. Available at: https://www.boehringer-ingelheim.ca/sites/ca/files/documents/viramunexrpmen.pdf. Accessed on 20 November 2022.

[3] I. Usach, V. Melis, J.E. Peris, Non-nucleoside reverse transcriptase inhibitors: a review on pharmacokinetics, pharmacodynamics, safety and tolerability, J. Int. AIDS Soc. 16 (2013) 18567, https://doi.org/10.7448/IAS.16.1.18567.

[4] A.M. Benedicto, I. Fuster-Martínez, J. Tosca, J.V. Esplugues, A. Blas-García, N. Apostolova, NNRTI and liver damage: evidence of their association and the mechanisms involved, Cells 10 (2021), https://doi.org/10.3390/cells10071687.

[5] C. Prasse, M.P. Schlüsener, R. Schulz, T.A. Ternes, Antiviral drugs in wastewater and surface waters: a new pharmaceutical class of environmental relevance? Environ. Sci. Technol. 44 (2010) 1728–1735, https://doi.org/10.1021/es903216p.

[6] A.O. Adeola, P.B.C. Forbes, Antiretroviral drugs in African surface waters: prevalence, analysis, and potential remediation, Environ. Toxicol. Chem. 41 (2022) 247–262, https://doi.org/10.1002/etc.5127.

[7] L. Yao, W.Y. Dou, Y.F. Ma, Y.S. Liu, Development and validation of sensitive methods for simultaneous determination of 9 antiviral drugs in different various environmental matrices by UPLC-MS/MS, Chemosphere 282 (2021), 131047, https://doi.org/10.1016/j.chemosphere.2021.131047.

[8] J.L. Wilkinson, A.B.A. Boxall, D.W. Kolpin, et al., Pharmaceutical pollution of the world's rivers, Proc. Natl. Acad. Sci. USA 119 (2022), e2113947119, https://doi.org/10.1073/pnas.2113947119.

[9] T.P. Wood, A.E. Basson, C. Duvenage, E.R. Rohwer, The chlorination behaviour and environmental fate of the antiretroviral drug nevirapine in South African surface water, Water Res. 104 (2016) 349–360, https://doi.org/10.1016/j.watres.2016.08.038.

[10] K. Sichilongo, M. Chinyama, A. Massele, S. Vento, Comparative chromatography–mass spectrometry studies on the antiretroviral drug nevirapine-analytical performance characteristics in human plasma determination, J. Chromatogr. B Biomed. Appl. 945-946 (2014) 101–109, https://doi.org/10.1016/j.jchromb.2013.11.046.

[11] I. Setayeshfar, H.R. Rajabi, O. Khani, Application of flow injection analysis-solid phase extraction based on ion-pair formation for selective preconcentration of trace amount of anti-HIV drug, Microchem. J. 177 (2022), 107245, https://doi.org/10.1016/j.microc.2022.107245.

[12] L.P. Fernández, R. Brasca, M.R. Alcaráz, M.J. Culzoni, High-throughput chemometrically assisted flow-injection method for the simultaneous determination of multi-antiretrovirals in water, Microchem. J. 141 (2018) 80–86, https://doi.org/10.1016/j.microc.2018.05.011.

[13] L.A. Filho, C.R. Galdez, C.A. Silva, M.F.M. Tavares, D.M. Costa, M.S. Aurora-Prado, Development and validation of a simple and rapid capillary zone electrophoresis method for determination of NNRTI nevirapine in pharmaceutical formulations, J. Braz. Chem. Soc. 22 (2011) 2005–2012, https://doi.org/10.1590/S0103-50532011001000024.

[14] B. Maganda, O. Heudi, A. Cortinovis, F. Picard, O. Kretz, O. Minzi, A fast and reliable reversed phase high performance liquid chromatography method for simultaneous determination of selected anti-retroviral and lumefantrine in human plasma, J. Chromatogr. B Biomed. Appl. 919-920 (2013) 52–60, https://doi.org/10.1016/j.jchromb.2013.01.009.

[15] L. Vieira-Sellaï, M. Quintana, O. Diop, O. Mercier, S. Tarrit, N. Raimi, A. Ba, B. Maunit, M.J. Galmier, Green HPLC quantification method of lamivudine, zidovudine and nevirapine with identification of related substances in tablets, Green Chem. Lett. Rev. 15 (2022) 695–704, https://doi.org/10.1080/17518253.2022.2129463.

[16] Y. Wu, J. Yang, C. Duan, L. Chu, S. Chen, S. Qiao, X. Li, H. Deng, Simultaneous determination of antiretroviral drugs in human hair with liquid chromatography-electrospray ionization-tandem mass spectrometry, J. Chromatogr. B Biomed. Appl. 1083 (2018) 209–221, https://doi.org/10.1016/j.jchromb.2018.03.021.

[17] O.A. Abafe, J. Späth, J. Fick, S. Jansson, C. Buckley, A. Stark, B. Pietruschka, B. S. Martincigh, LC-MS/MS determination of antiretroviral drugs in influents and effluents from wastewater treatment plants in KwaZulu-Natal, South Africa, Chemosphere 200 (2018) 660–670, https://doi.org/10.1016/j.chemosphere.2018.02.105.

[18] S. Notari, C. Mancone, T. Alonzi, M. Tripodi, P. Narciso, P. Ascenzi, Determination of abacavir, amprenavir, didanosine, efavirenz, nevirapine, and stavudine concentration in human plasma by MALDI-TOF/TOF, J. Chromatogr. B Biomed. Appl. 863 (2008) 249–257, https://doi.org/10.1016/j.jchromb.2008.01.009.

[19] L. Li, Y. Cheng, Y. Ding, Y. Lu, F. Zhang, Application of thioglycolic acid capped nano-ZnS as a fluorescence probe for the determination of nevirapine, Anal. Methods 4 (2012) 4213–4219, https://doi.org/10.1039/C2AY26002F.

[20] K.V. Mokwebo, S.F. Douman, O.V. Uhuo, K.C. Januarie, M. Oranzie, E.I. Iwuoha, Electroanalytical sensors for antiretroviral drugs determination in pharmaceutical and biological samples: a review, J. Electroanal. Chem. 920 (2022), 116621, https://doi.org/10.1016/j.jelechem.2022.116621.

[21] S.A. Ozkan, J.M. Kauffmann, P. Zuman, Electroanalysis in Biomedical and Pharmaceutical Sciences, Voltammetry, Amperometry, Biosensors, Applications, Springer, Berlin, Heidelberg, 2015, p. 350.

[22] S. Shahrokhian, R. Kohansal, M. Ghalkhani, M.K. Amini, Electrodeposition of copper oxide nanoparticles on precasted carbon nanoparticles film for electrochemical investigation of anti-HIV drug nevirapine, Electroanalysis 27 (2015) 1989–1997, https://doi.org/10.1002/elan.201500027.

[23] K. Kantize, I.N. Booysen, A. Mambanda, Electrocatalytic determination of nevirapine using a platinum electrode modified with a polymeric CoPc-Nafion-carbon nanotube composite, Int. J. Electrochem. Sci. 17 (2022), https://doi.org/10.20964/2022.06.03.

[24] F. Zhang, L. Li, L. Luo, Y. Ding, X. Liu, Electrochemical oxidation and determination of antiretroviral drug nevirapine based on uracil-modified carbon paste electrode, J. Appl. Electrochem. 43 (2013) 263–269, https://doi.org/10.1007/s10800-012-0516-z.

[25] M.B. Gholivand, E. Ahmadi, M. Haseli, A novel voltammetric sensor for nevirapine, based on modified graphite electrode by MWCNs/poly(methylene blue)/gold nanoparticle, Anal. Biochem. 527 (2017) 4–12, https://doi.org/10.1016/j.ab.2017.03.018.

[26] E. Ahmadi, M.R. Eyvani, V. Riahifar, H. Momeneh, C. Karami, Amperometric determination of nevirapine by GCE modified with c-MWCNTs and synthesized 11-mercaptoundecanoyl hydrazinecarbothioamide coated silver nanoparticles, Microchem. J. 146 (2019) 1218–1226, https://doi.org/10.1016/j.microc.2019.02.054.

[27] N.L. Teradal, J. Seetharamappa, Bulk modification of carbon paste electrode with Bi2O3 nanoparticles and its application as an electrochemical sensor for selective sensing of anti-HIV drug nevirapine, Electroanalysis 27 (2015) 2007–2016, https://doi.org/10.1002/elan.201500088.

[28] M.M. Foroughi, S. Jahani, Z. Aramesh-Boroujeni, M. Rostaminasab Dolatabad, K. Shahbazkhani, Synthesis of 3D cubic of Eu3+/Cu2O with clover-like faces nanostructures and their application as an electrochemical sensor for determination of antiretroviral drug nevirapine, Ceram. Int. 47 (2021) 19727–19736, https://doi.org/10.1016/j.ceramint.2021.03.311.

[29] P. Tiwari, N.R. Nirala, R. Prakash, Determination of the anti-HIV drug nevirapine using electroactive 2D material Pd@rGO decorated with MoS2 quantum dots, ChemistrySelect 3 (2018) 5341–5347, https://doi.org/10.1002/slct.201702250.

[30] F.O. Okumu, B. Silwana, M.C. Matoetoe, Application of MWCNT/Ag-Pt nanocomposite modified GCE for the detection of nevirapine in pharmaceutical formulation and biological samples, Electroanalysis 32 (2020) 3000–3008, https://doi.org/10.1002/elan.202060374.

[31] D. Apath, M. Moyo, M. Shumba, TiO2 nanoparticles decorated graphene nanoribbons for voltammetric determination of an anti-HIV drug nevirapine, J. Chem. 2020 (2020), 3932715, https://doi.org/10.1155/2020/3932715.
[32] S. Massumi, E. Ahmadi, A. Akbari, M.B. Gholivand, Highly sensitive and selective sensor based on molecularly imprinted polymer for voltammetric determination of nevirapine in biological samples, J. Electroanal. Chem. 876 (2020), 114508, https://doi.org/10.1016/j.jelechem.2020.114508.
[33] B. Hassan Pour, N. Haghnazari, F. Keshavarzi, E. Ahmadi, B.R. Zarif, A sensitive sensor based on molecularly imprinted polypyrrole on reduced graphene oxide modified glassy carbon electrode for nevirapine analysis, Anal. Methods 13 (2021) 4767–4777, https://doi.org/10.1039/D1AY00500F.
[34] K. Cinková, Ľ. Švorc, P. Šatkovská, M. Vojs, P. Michniak, M. Marton, Simple and rapid quantification of folic acid in pharmaceutical tablets using a cathodically pretreated highly boron-doped polycrystalline diamond electrode, Anal. Lett. 49 (2016) 107–121, https://doi.org/10.1080/00032719.2014.999272.
[35] Z. Chomisteková, E. Culková, R. Bellová, D. Melicherčíková, J. Durdiak, J. Timko, M. Rievaj, P. Tomčík, Oxidation and reduction of omeprazole on boron-doped diamond electrode: mechanistic, kinetic and sensing performance studies, Sens. Actuators B Chem. 241 (2017) 1194–1202, https://doi.org/10.1016/j.snb.2016.10.014.
[36] C.P. Sousa, F.W.P. Ribeiro, T.M.B.F. Oliveira, G.R. Salazar-Banda, P. de Lima-Neto, S. Morais, A.N. Correia, Electroanalysis of pharmaceuticals on boron-doped diamond electrodes: a review, ChemElectroChem 6 (2019) 2350–2378, https://doi.org/10.1002/celc.201801742.
[37] M. Yence, A. Cetinkaya, G. Ozcelikay, S.I. Kaya, S.A. Ozkan, Boron-doped diamond electrodes: recent developments and advances in view of electrochemical drug sensors, Crit. Rev. Anal. Chem. 52 (2022) 1122–1138, https://doi.org/10.1080/10408347.2020.1863769.
[38] S. Baluchová, J. Barek, L.I.N. Tomé, C.M.A. Brett, K. Schwarzová-Pecková, Vanillylmandelic and Homovanillic acid: electroanalysis at non-modified and polymer-modified carbon-based electrodes, J. Electroanal. Chem. 821 (2018) 22–32, https://doi.org/10.1016/j.jelechem.2018.03.011.
[39] K. Asai, T.A. Ivandini, M.M. Falah, Y. Einaga, Surface termination effect of boron-doped diamond on the electrochemical oxidation of adenosine phosphate, Electroanalysis 28 (2016) 177–182, https://doi.org/10.1002/elan.201500505.
[40] Z. Liu, A.F. Sartori, J.G. Buijnsters, Role of sp^2 carbon in non-enzymatic electrochemical sensing of glucose using boron-doped diamond electrodes, Electrochem. Commun. 130 (2021), 107096, https://doi.org/10.1016/j.elecom.2021.107096.
[41] Ľ. Švorc, K. Kalcher, Modification-free electrochemical approach for sensitive monitoring of purine DNA bases: simultaneous determination of guanine and adenine in biological samples using boron-doped diamond electrode, Sens. Actuators B Chem. 194 (2014) 332–342, https://doi.org/10.1016/j.snb.2013.12.104.
[42] Ľ. Švorc, K. Cinková, A. Samphao, D.M. Stanković, E. Mehmeti, K. Kalcher, Voltammetric determination of harmaline in natural food products using boron-doped diamond electrode, J. Electroanal. Chem. 744 (2015) 37–44, https://doi.org/10.1016/j.jelechem.2015.03.004.
[43] O. Sarakhman, Ľ. Švorc, A review on recent advances in the applications of boron-doped diamond electrochemical sensors in food analysis, Crit. Rev. Anal. Chem. 52 (2022) 791–813, https://doi.org/10.1080/10408347.2020.1828028.
[44] P. Joshi, P. Riley, K.Y. Goud, R.K. Mishra, R. Narayan, Recent advances of boron-doped diamond electrochemical sensors toward environmental applications, Curr. Opin. Electrochem. 32 (2022), 100920, https://doi.org/10.1016/j.coelec.2021.100920.
[45] L. Bandžuchová, Ľ. Švorc, M. Vojs, M. Marton, P. Michniak, J. Chýlková, Self-assembled sensor based on boron-doped diamond and its application in voltammetric analysis of picloram, Int. J. Environ. Anal. Chem. 94 (2014) 943–953, https://doi.org/10.1080/03067319.2013.879300.
[46] S. Baluchová, A. Daňhel, H. Dejmková, V. Ostatná, M. Fojta, K. Schwarzová-Pecková, Recent progress in the applications of boron doped diamond electrodes in electroanalysis of organic compounds and biomolecules – a review, Anal. Chim. Acta 1077 (2019) 30–66, https://doi.org/10.1016/j.aca.2019.05.041.
[47] N. Yang, S. Yu, J.V. Macpherson, Y. Einaga, H. Zhao, G. Zhao, G.M. Swain, X. Jiang, Conductive diamond: synthesis, properties, and electrochemical applications, Chem. Soc. Rev. 48 (2019) 157–204, https://doi.org/10.1039/C7CS00757D.
[48] J.V. Macpherson, A practical guide to using boron doped diamond in electrochemical research, Phys. Chem. Chem. Phys. 17 (2015) 2935–2949, https://doi.org/10.1039/c4cp04022h.
[49] K. Schwarzová-Pecková, J. Vosáhlová, J. Barek, I. Šloufová, E. Pavlova, V. Petrák, J. Zavázalová, Influence of boron content on the morphological, spectral, and electroanalytical characteristics of anodically oxidized boron-doped diamond electrodes, Electrochim. Acta 243 (2017) 170–182, https://doi.org/10.1016/j.electacta.2017.05.006.
[50] S. Baluchová, A. Taylor, V. Mortet, S. Sedláková, L. Klimša, J. Kopeček, O. Hák, K. Schwarzová-Pecková, Porous boron doped diamond for dopamine sensing: effect of boron doping level on morphology and electrochemical performance, Electrochim. Acta 327 (2019), 135025, https://doi.org/10.1016/j.electacta.2019.135025.
[51] T.A. Ivandini, T. Watanabe, T. Matsui, Y. Ootani, S. Iizuka, R. Toyoshima, H. Kodama, H. Kondoh, Y. Tateyama, Y. Einaga, Influence of surface orientation on electrochemical properties of boron-doped diamond, J. Phys. Chem. C 123 (2019) 5336–5344, https://doi.org/10.1021/acs.jpcc.8b10406.
[52] A. Taylor, S. Baluchová, L. Fekete, L. Klimša, J. Kopeček, D. Šimek, M. Vondráček, L. Míka, J. Fischer, K. Schwarzová-Pecková, V. Mortet, Growth and comparison of high-quality MW PECVD grown B doped diamond layers on {118}, {115} and {113} single crystal diamond substrates, Diam. Relat. Mater. 123 (2022), 108815, https://doi.org/10.1016/j.diamond.2021.108815.
[53] Z. Liu, S. Baluchová, A.F. Sartori, Z. Li, Y. Gonzalez-Garcia, M. Schreck, J. G. Buijnsters, Heavily boron-doped diamond grown on scalable heteroepitaxial quasi-substrates: a promising single crystal material for electrochemical sensing applications, Carbon 201 (2023) 1229–1240, https://doi.org/10.1016/j.carbon.2022.10.023.
[54] M.C. Granger, G.M. Swain, The influence of surface interactions on the reversibility of ferri/ferrocyanide at boron-doped diamond thin-film electrodes, J. Electrochem. Soc. 146 (1999) 4551, https://doi.org/10.1149/1.1392673.
[55] N. Alpar, Y. Yardım, Z. Şentürk, Selective and simultaneous determination of total chlorogenic acids, vanillin and caffeine in foods and beverages by adsorptive stripping voltammetry using a cathodically pretreated boron-doped diamond electrode, Sens. Actuators B Chem. 257 (2018) 398–408, https://doi.org/10.1016/j.snb.2017.10.100.
[56] R. Trouillon, Y. Einaga, M.A.M. Gijs, Cathodic pretreatment improves the resistance of boron-doped diamond electrodes to dopamine fouling, Electrochem. Commun. 47 (2014) 92–95, https://doi.org/10.1016/j.elecom.2014.07.028.
[57] Z. Deng, R. Zhu, L. Ma, K. Zhou, Z. Yu, Q. Wei, Diamond for antifouling applications: a review, Carbon 196 (2022) 923–939, https://doi.org/10.1016/j.carbon.2022.05.015.
[58] H. Girard, N. Simon, D. Ballutaud, M. Herlem, A. Etcheberry, Effect of anodic and cathodic treatments on the charge transfer of boron doped diamond electrodes, Diam. Relat. Mater. 16 (2007) 316–325, https://doi.org/10.1016/j.diamond.2006.06.009.
[59] S. Yu, S. Liu, X. Jiang, N. Yang, Recent advances on electrochemistry of diamond related materials, Carbon 200 (2022) 517–542, https://doi.org/10.1016/j.carbon.2022.09.044.
[60] T.A. Enache, A.M. Chiorcea-Paquim, O. Fatibello-Filho, A.M. Oliveira-Brett, Hydroxyl radicals electrochemically generated *in situ* on a boron-doped diamond electrode, Electrochem. Commun. 11 (2009) 1342–1345, https://doi.org/10.1016/j.elecom.2009.04.017.
[61] B.C. Lourencao, R.F. Brocenschi, R.A. Medeiros, O. Fatibello-Filho, R.C. Rocha-Filho, Analytical applications of electrochemically pretreated boron-doped diamond electrodes, ChemElectroChem 7 (2020) 1291–1311, https://doi.org/10.1002/celc.202000050.
[62] L.A. Hutton, J.G. Iacobini, E. Bitziou, R.B. Channon, M.E. Newton, J. V. Macpherson, Examination of the factors affecting the electrochemical performance of oxygen-terminated polycrystalline boron-doped diamond electrodes, Anal. Chem. 85 (2013) 7230–7240, https://doi.org/10.1021/ac401042t.
[63] S. Kasahara, K. Natsui, T. Watanabe, Y. Yokota, Y. Kim, S. Iizuka, Y. Tateyama, Y. Einaga, Surface hydrogenation of boron-doped diamond electrodes by cathodic reduction, Anal. Chem. 89 (2017) 11341–11347, https://doi.org/10.1021/acs.analchem.7b02129.
[64] H. Parham, B. Zargar, Determination of isosorbide dinitrate in arterial plasma, synthetic serum and pharmaceutical formulations by linear sweep voltammetry on a gold electrode, Talanta 55 (2001) 255–262, https://doi.org/10.1016/S0039-9140(01)00416-7.
[65] M. Wang, N. Simon, C. Decorse-Pascanut, M. Bouttemy, A. Etcheberry, M. Li, R. Boukherroub, S. Szunerits, Comparison of the chemical composition of boron-doped diamond surfaces upon different oxidation processes, Electrochim. Acta 54 (2009) 5818–5824, https://doi.org/10.1016/j.electacta.2009.05.037.
[66] I. Yagi, H. Notsu, T. Kondo, D.A. Tryk, A. Fujishima, Electrochemical selectivity for redox systems at oxygen-terminated diamond electrodes, J. Electroanal. Chem. 473 (1999) 173–178, https://doi.org/10.1016/S0022-0728(99)00027-3.
[67] Y. Wang, J.G. Limon-Petersen, R.G. Compton, Measurement of the diffusion coefficients of $[Ru(NH_3)_6]^{3+}$ and $[Ru(NH_3)_6]^{2+}$ in aqueous solution using microelectrode double potential step chronoamperometry, J. Electroanal. Chem. 652 (2011) 13–17, https://doi.org/10.1016/j.jelechem.2010.12.011.
[68] K.B. Holt, A.J. Bard, Y. Show, G.M. Swain, Scanning electrochemical microscopy and conductive probe atomic force microscopy studies of hydrogen-terminated boron-doped diamond electrodes with different doping levels, J. Phys. Chem. B 108 (2004) 15117–15127, https://doi.org/10.1021/jp048222x.
[69] R. Bogdanowicz, J. Ryl, Structural and electrochemical heterogeneities of boron-doped diamond surfaces, Curr. Opin. Electrochem. 31 (2022), 100876, https://doi.org/10.1016/j.coelec.2021.100876.
[70] Chemicalize. Available at: https://chemicalize.com/acpp/calculation. Accessed on 05 November 2022.
[71] E. Laviron, General expression of the linear potential sweep voltammogram in the case of diffusionless electrochemical systems, J. Electroanal. Chem. 101 (1979) 19–28, https://doi.org/10.1016/S0022-0728(79)80075-3.
[72] Q. Li, C. Batchelor-McAuley, R.G. Compton, Electrochemical oxidation of guanine: electrode reaction mechanism and tailoring carbon electrode surfaces to switch between adsorptive and diffusional responses, J. Phys. Chem. B 114 (2010) 7423–7428, https://doi.org/10.1021/jp1021196.
[73] S. Siraj, C.R. McRae, D.K.Y. Wong, Hydrogenating carbon electrodes by n-butylsilane reduction to achieve an antifouling surface for selective dopamine detection, Sens. Actuators B Chem. 327 (2021), 128881, https://doi.org/10.1016/j.snb.2020.128881.
[74] A.F. Hagel, H. Albrecht, W. Dauth, W. Hagel, F. Vitali, I. Ganzleben, H.W. Schultis, P.C. Konturek, J. Stein, M.F. Neurath, M. Raithel, Plasma concentrations of

ascorbic acid in a cross section of the German population, Int. J. Med. Res. 46 (2018) 168–174, https://doi.org/10.1177/0300060517714387.
[75] M. Dório, I.M. Benseñor, P. Lotufo, I.S. Santos, R. Fuller, Reference range of serum uric acid and prevalence of hyperuricemia: a cross-sectional study from baseline data of ELSA-Brasil cohort, Adv. Rheumatol. 62 (2022) 15, https://doi.org/10.1186/s42358-022-00246-3.
[76] P. Fan-Havard, Z.F. Liu, M. Chou, Y.H. Ling, A. Barrail-Tran, D.W. Haas, A. M. Taburet, A.S. Grp, Pharmacokinetics of phase I nevirapine metabolites following a single dose and at steady state, Antimicrob. Agents Chemother. 57 (2013) 2154–2160, https://doi.org/10.1128/AAC.02294-12.